Transmembrane Signaling Regulates the Remodeling of the Actin Cytoskeleton: Roles of PKC and Adducin

Bih-Hwa Shieh, Wesley Sun and Darwin Ferng

From the Department of Pharmacology, Center for Molecular Neuroscience and Vision Research Center, Vanderbilt University, Nashville, TN 37232, USA

Correspondence should be addressed to Dr. Bih-Hwa Shieh, Vanderbilt University, Department of Pharmacology, 402 Robinson Research Building, Nashville, TN 37232. Telephone: (615)-343-0441; FAX: (615)-343-6532; Email: bih-hwa.shieh@vanderbilt.edu

Abbreviations:

Aa, amino acids; Arr2, arrestin 2; DAG, diacylglycerol; dpp, deep pseudopupil; hts, hu-li tai shao; inaC, inactivation-no-afterpotential C; INAD, inactivation-no-afterpotential D; MARCKS, myristoylated alanine-rich C-kinase substrate; NorpA, no-receptor potential A; PKC, protein kinase C; PLC phospholipase C: RNAi, RNA interference; RT/PCR, reverse transcription/polymerase chain reaction; TRP, transient receptor potential; TRPL, TRP-like

Abstract

Members of the conventional protein kinase C (cPKC) family are activated by both DAG and Ca^{2+} and have been implicated in the regulation of the actin cytoskeleton. *Drosophila* contains two cPKC's, Pkc53E (Pkc1) and eye-PKC (Pkc2); mutants missing each PKC lead to retinal degeneration. While eye-PKC is critical for the visual signaling, the role of Pkc53E is not known. We identified a photoreceptor-specific isoform of Pkc53E and show Pkc53E-RNAi negatively impacts the actin cytoskeleton of rhabdomeres. Interestingly, Pkc53E-RNAi enhances the degeneration of $norpA^{P24}$ photoreceptors, suggesting Pkc53E could be activated independently of NorpA/PLCβ4. We further demonstrate that in $norpA^{P24}$ photoreceptors Plc21C can be activated by Gq, which is responsible for the activation of Pkc53E. We explored whether Pkc53E regulates adducin in *Drosophila* photoreceptors. Adducin cross-links the actin cytoskeleton to the spectrin network, which is blunted by PKC phosphorylation. Importantly, we observed that phosphorylation of adducin was greatly reduced in a null allele of *pkc53E*. Downregulation of *hts* that encodes *Drosophila* adducin, exerts a more severe effect than Pkc53E-RNAi to impact the actin cytoskeleton. In contrast, overexpression of a mCherry tagged *Add2,* one of the three *Drosophila* adducin isoforms, led to the apical expansion of rhabdomeres with overgrowth of the actin cytoskeleton. This phenotype is likely caused by the dominant-negative activity of the tagged Add2 as it also was observed in α-spectrin-RNAi or β-spectrin-RNAi. Interestingly, downregulation of Pkc53E does not suppress the expansion of rhabdomeres during development, but negatively affects the appearance of rhabdomeres in adult photoreceptors. We conclude that *Drosophila* adducin has two distinct functions: in pupal photoreceptors, it regulates rhabdomere morphogenesis, which is independent of Pkc53E. In adult photoreceptors, it promotes the maintenance of the actin cytoskeleton, which is regulated by Pkc53E in response to the light-induced activation of the PLCβ activity.

Introduction

Conventional protein kinase C (cPKC) is a target of phorbol esters and is activated by diacylglycerol (DAG) and Ca^{2+} (Lipp and Reither, 2011). cPKC is a downstream mediator following the activation of phospholipase C (PLC) that includes PLCβ and PLCγ. PLCγ is activated following the stimulation of growth factor receptors, and cPKC's such as PKCα, PKCβI, PKCβII, and PKCγ, have been shown critical for processes associated with morphological changes leading to growth and differentiation of cells. In contrast, in PLCβ mediated signaling events such as the visual signaling that takes place in *Drosophila* compound eyes, in which rhodopsin couples to the heterotrimeric Gq protein leading to the activation of PLCβ4 (NorpA) (Hardie and Juusola, 2015; Montell, 2012), the role of cPKC in regulating cell morphology is less explored. cPKC has been commonly linked to the regulation of the actin cytoskeleton (Larsson, 2006). Indeed, several PKC substrates have been identified and characterized. However, the mechanisms by which cPKC regulates cell morphology or the cytoskeleton remain to be explored.

There are two cPKC's that are expressed in *Drosophila* photoreceptors, eye-PKC (Schaeffer et al., 1989) and Pkc53E (Rosenthal et al., 1987), both of which share over 70% sequence identities. Both genes are located in tandem in the second chromosome and may arise by gene duplication. Eye-PKC is preferentially expressed in photoreceptors and is localized in the rhabdomere (Smith et al., 1991), the visual organelle in which the visual signaling takes place. Moreover, eye-PKC is an integral part of the multimeric signaling complex organized by the scaffolding protein INAD (inactivation-no-afterpotential D) that directly associates with eye-PKC, NorpA, and the TRP Ca^{2+} channel (Adamski et al., 1998; Tsunoda and Zuker, 1999). Eye-PKC has been shown to phosphorylate both INAD and TRP (transient receptor potential) in the complex (Peng et al., 2008; Popescu et al., 2006). In contrast, the role of Pkc53E has not been investigated. The *pkc53E* gene gives rise to multiple transcripts including some that are present in photoreceptors.

Studies in cell cultures have linked cPKC to the regulation of the actin cytoskeleton (Larsson, 2006). The actin cytoskeleton consists of a network of actin filaments in which filamentous F-actin are intertwined to form actin microfilaments, which can be found in the cell cortex, the stress fiber, and various extensions including filopodia, lamellipodia, and microvilli. The actin cytoskeleton is critical not only for maintaining cell shape but also for diverse

processes including endocytosis, cytokinesis, and chemotaxis, and consequently, is dynamically regulated (Schmidt and Hall, 1998). In the cell cortex, actin microfilaments support the plasma membrane by forming the membrane scaffold with the spectrin network (Baines, 2010). Moreover, the interaction between spectrin and actin filaments is dynamically regulated by adducin (Baines, 2010), a family of cytoskeletal proteins consisting of three adducins (α-, β- and γ-adducin) (Joshi et al., 1991). Importantly, adducins are regulated by Ca^{2+} and by the second messenger regulated protein kinases including PKC as adducins contain the sequence related to the conserved MARCKS (myristoylated alanine-rich C-kinase substrate) domain. For example, activation by par ligands or phorbol esters in platelets results in PKC phosphorylation of adducin, which leads to its dissociation from spectrin and actin (Barkalow et al., 2003). The release of phosphorylated adducin from the barbed end of the actin filament would promote actin polymerization. Thus, adducin acts as a key regulatory protein to initiate remodeling of the actin cytoskeleton following an increase of the intracellular Ca^{2+} and activation of PKC. Pkc53E may regulate adducin to orchestrate reorganization of the actin cytoskeleton to ensure the maintenance of rhabdomeres following the activation of the visual signaling.

Here we identified a photoreceptor-specific isoform of Pkc53E, Pkc53E-B, and show that downregulation of Pkc53E-B leads to a loss of rhabdomeres possibly by affecting the actin cytoskeleton. We explored the regulation by the visual signaling and observed Pkc53E was partially active in the absence of PLCβ4 /NorpA. Indeed, we show a second PLCβ in the eye, Plc21C (Shortridge et al., 1991), can be activated by Gq when NorpA is absent leading to the activation of Pkc53E. We investigated whether Pkc53E regulates *Drosophila* adducin or Hts (hu-li tai shao) (Yue and Spradling, 1992) and show that phosphorylation of adducin at the conserved PKC phosphorylation site was greatly reduced in a *pkc53E* null allele. Moreover, similar to Pkc53E-RNAi, downregulation of adducin expression by RNAi also results in loss of rhabdomeres. In contrast, overexpression of a tagged adducin in photoreceptors leads to apical expansion of rhabdomeres similar to knockdown of spectrins, supporting the notion that adducin plays a critical role in rhabdomere morphogenesis during pupal development. Unexpectedly, the apical expansion is not perturbed by downregulation or overexpression of *pkc53E*. We conclude that Pkc53E regulates adducin for the maintenance of the actin cytoskeleton in adult photoreceptors.

Materials and Methods

Fluorescence microscopy

Adult flies were anesthetized by CO_2, immobilized in clay with compound eyes facing upward in a 50 mm Petri dish for imaging. The compound eye was examined using an upright Olympus AX70 microscope equipped with a 10X lens (for detecting deep pseudopupil) or 40X (LUMPlan 40X) or 100X (LUMPlan 100X) water immersion lens for examining multiple ommatidia. Image acquisition was performed at 100X magnification for dpp and 400X or 1000X for rhabdomeres/ommatidia using IPLab image acquisition software (BioVision Technologies, Exton, PA, USA) and the Retiga camera from QImaging (Surrey, BC, Canada). Exposure time was made constant throughout each experiment based on the brightest signal in the control group. Multiple flies ($n \geq 3$) of each genotype were analyzed.

Fly handling for microscopy

Adult flies were sorted and manipulated under a dissecting microscope with a light source of 600 lux for less than one minute. During imaging, compound eyes were subjected to the blue light (1300 lux) or green light (4500 lux) from the fluorescent microscope, and images were taken immediately for Actin-GFP, Arr2-GFP, or Rh1-mCherry.

Fluorescent image analysis

All image manipulation was performed under the guideline of Rossner and Yamada (Rossner and Yamada, 2004). Fluorescent images included in the Figures are similar in appearance to the raw images. Experimentally, we collected newly eclosed flies of the desirable genotype, placed them in a vial, and aged at 25 °C in a 12h light/dark cycle (ambient light 300 lux) for various amounts of time. Flies were analyzed for GFP-marked rhabdomeres by water-immersion fluorescence microscopy. Retinal morphology was scored based on the number of rhabdomeres present in a given ommatidium (unit eye) similar to that described by Cerny et al. (2013). Briefly, retinas from three flies from each eight ommatidia were counted to obtain the average of the rhabdomere number. To score rhabdomere

areas, ImageJ was used. Four ommatidia clusters were selected in which the total rhabdomere area of each cluster was measured and averaged. Wild-type flies of the same age were used as controls.

Quantitative Western blotting

Single fly head or four retinas was dissected and extracted with 15 μl of 2X Laemmli sample buffer by sonication. Protein extracts were size-fractionated by SDS/PAGE (10-12%) and transferred onto a nitrocellulose filter. Filters were incubated with desired primary antibodies, followed by the fluorophore-conjugated secondary antibodies (IRDye 680LT Goat anti-Rabbit IgG, or IRDye 800CW Goat anti-mouse IgG, LI-COR). The fluorophore signal was detected by the Odyssey Infrared Imaging System (LI-COR, Lincoln, NE, USA), and analyzed by Image Studio™ 5.2.

Individual protein content was normalized by comparing it to the loading control (actin or fascin). We carried out three to five analyses (n = 3-5) with each using one fly head or four retinas. Polyclonal antibodies against Gq α-subunit were generated in rabbits using a bacterial fusion protein corresponding to 1-200 aa of Gq. Polyclonal anti-phospho-$Ser^{726/705/703}$ adducin antibodies were purchased from Millipore (Burlington, MA, USA). Monoclonal antibodies for Rh1 (4C5), TRP (MAb83F6), adducin/Hts (1B1), actin (JLA20), and fascin (sn_7C) were obtained from Developmental Studies Hybridoma Bank (University of Iowa).

Recombinant DNA and Molecular Biology A full-length Rh1 cDNA without the stop codon was generated by PCR with the engineered SacI (5') and EcoRI (3') restriction enzyme sites. The mCherry cDNA sequence with the flanking EcoRI (5') and XhoI (3') restriction enzyme sites was generated by PCR using pUAST-mCherry [a gift from Dr. Amy Kiger (UCSD)] as the template. The mCherry nucleotide sequence was inserted in-frame into the 3' of the Rh1 cDNA and the resulting Rh1-mCherry chimera DNA was subcloned into YC4 for the expression under the control of the *Drosophila* Rh1 promoter (Kristaponyte et al., 2012).

Reverse Transcription-Polymerase Chain Reaction (RT-PCR)

Total RNA was extracted from 20 fly heads (or 50 retinas) by a modified method of Chirqwin et al (1979) and dissolved in 20 μl water. Five microliter (μl) of total RNA were used for the first-strand cDNA synthesis via Superscript III (Invitrogen, Carlsbad, CA) primed with random hexamers. Quantitative PCR in triplicate was performed via CFX96 Real-Time System (BIO-RAD, Hercules, CA) using iQTM SYBR Green Supermix (BIO-RAD). All expression values were normalized to RpL32 (rp49). To compare isoform specific transcript in various genetic backgrounds, RT/PCR products were analyzed by 8% polyacrylamide gel and relative band intensity was quantified using Image Lab (Bio-Rad). Most of the primer sequences used were selected from the FlyPrimerBank (Hu et al., 2013) and listed below: *rp49* (113 nt), AGCATACAGGCCCAAGATCG (5'), TGTTGTCGATACCCTTGGGC (3'); *Pkc53E* (for total *Pkc53E*, 90nt), AGACTCGCACCATTAAGGCTT (5'), GGATGCGTCGATCCTTGTCTT (3'); *Pkc53E* (for distinguishing between C/E/B, 356/359 nt and A/F, 332 nt), CACGTTCTGCTCCCACTGCA (5'), GCTCCGTGTGATCGCATCC (3'); *Pkc53E* (for F, 262 nt or B, 289 nt), AGCCCTCAAGAAGAAGAACGT (5'), TCCTGCGTATGTGAATGGCTC (3'); *Pkc53E* for C/E (282 nt) AGCCCTCAAGAAGAAGAACGT (5'), AGGAAGGTGACATTCTGCCA (3'); *α-spectrin* (205 nt), GGTTCTGTCCCGCTACAATG (5'), TCGAACGCCTGATGTTTCTGG (3'); *β-spectrin* (121 nt) CCGCATTGCCGATCTCTATGT (5'), CAGGCAGTGGATACGCATCTT (3'); *karst* (182 nt), GTCGGAGAAACTGGGCAAG (5'), GAAACCGCAGAATGATGGTCC (3'); *arr1* (90 nt), CATGAACAGGCGTGATTTTGTAG (5'), TTCTGGCGCACGTACTCATC (3'); *Plc21C* (159 nt), GAGAAGACAGTGACGGTATGC (5'), CAGGAACATAATCGCCGAGC (3'). Primers specifically for isoforms I/L/M are AGAGCAGTAAAGAGTTCCAG (5') and GGCCTCGGCCTTCTTCTTC(3'), for isoforms O/S are CAGAGCAGTAAAGAGGATGTC (5') and GGCCTCGGCCTTCTTCTTC(3'). Primers for distinguishing between Q/R or O/S are CCACAAAGCGAACCCGAGA (5') and GACATCCTCTTTACTGCTCTG (3').

Drosophila stocks

Drosophila lines including mutants for eye-PKC (*inaC*^{P209}, #42241), and *Pkc53E* (*Pkc53E*$^{\Delta 28}$, #80988) were obtained from Bloomington Drosophila Stock Center (BDSC) (NIH P40OD018537). Transgenic flies for GMR-GAL4 (stock #1104), RNAi lines for the following genes including *hts* (#35421), *α-spectrin* (#48201), *β-spectrin* (#48202), *spectrin-βH* or *karst* (#33933) , *inaC* (#36776), *Pkc53E* (#55864), *Gαq* (#63987), and *plc21C*(#31269, #33719) were also obtained from BDSC. UAS-driven overexpressing lines including *hts-mCherry* (#66171), *Pkc53E-B* (#80989), and Actin-GFP (#9253) were from BDSC. Fly cultures were maintained in the standard cornmeal medium at 25 °C. Standard crosses were used to introduce suitable genetic backgrounds.

Statistical analysis

One-way ANOVA and two-tailed Student's *t*-test were employed for statistical analysis.

Results

Characterization of a *pkc53E* null allele and identification of a photoreceptor-specific Pkc53E isoform

In *Drosophila* photoreceptors, activation of rhodopsin leads to a transient rise of cytoplasmic Ca^{2+}, which has been implicated in regulating the visual response and in maintaining the structural integrity of photoreceptors (Voolstra and Huber, 2020). The Ca^{2+} transient thereby activates several protein kinases including the Ca^{2+}/calmodulin-dependent protein kinase II and PKC. In the *Drosophila* genome, there are two conventional PKC's, eye-PKC and Pkc53E, both of which are expressed in the eye. Specifically, eye-PKC has been shown to phosphorylate and regulate TRP (Peng et al., 2008; Popescu et al., 2006; Voolstra et al., 2013), and mutants lacking eye-PKC (*inaC*) display abnormal visual signaling and retinal degeneration (Hardie et al., 1993; Ranganathan et al., 1991; Smith et al., 1991). In contrast, the role of Pkc53E in the eye has not been investigated. We explored whether Pkc53E promotes the survival of photoreceptors.

First, we characterized a null allele of *pkc53E*, $pkc53E^{\Delta 28}$ (Figure S1), and show it displays light-dependent retinal degeneration that is accompanied by a reduction of Rh1(Figure 1A). The loss of Rh1 is less severe compared to a null allele of eye-PKC ($inaC^{P209}$). Indeed, seven-day-old $pkc53E^{\Delta 28}$ contained about 47.8$\pm$6.1% (n = 4) of Rh1, while $inaC^{P209}$, 14.8$\pm$2.5% (n = 4), based on Western blotting.

Next, we investigated the critical Pkc53E isoform in photoreceptors. The *pkc53E* gene encodes six transcripts (RA-F) leading to the translation of four distinct polypeptides, which include isoforms of 679 amino acids (aa) (PB), 678 aa (PC, PE), 670 aa (PA, PF), and 525 aa (PD), with different N-terminal sequences (Figure 1B). Specifically, all isoforms contain the C2 domain for the Ca^{2+} binding and all also contain two C1 domains that bind to DAG, except PD (Figure 1C). The PD isoform lacks the N-terminal 145 aa and therefore its activity is likely independent of DAG. DAG may exert different affinity towards PA and PF isoforms as both are missing eight amino acids in the first C1 domain when compared to the PB, PC, and PE isoforms (Figure 1C). Taken together, these Pkc53E isoforms have distinct C1 domains, which contribute to the activation and activity of each isoform.

We investigated which *pkc53E* isoforms are expressed in photoreceptors via RT/PCR (Figure 1D). Using oligonucleotide primers flanking or at the alternative spliced sites, we demonstrate that mRNA coding for the isoform

B/C/E group is present in wild-type (Figure 1D, lane 8) but greatly reduced in heads of *glass* mutants lacking photoreceptors (Moses et al., 1989) (lane 7). This result supports that the group of the B/C/E transcripts is preferentially expressed in photoreceptors. To explore further, we observed that transcripts for the C/E group are present at a low level in both wild-type and *glass* heads (Figure 1D, lanes 3 and 4). In contrast, mRNA for the B isoform is highly expressed in wild-type (Figure 1D, lane 10) but not *glass* heads (lane 9). Taken together, we conclude that *pkc53E-B* that encodes a protein of 679 aa is preferentially expressed in photoreceptors.

Downregulation of either Pkc53E or eye-PKC leads to retinal degeneration via two GFP reporters

To investigate the role of Pkc53E-B in photoreceptors, we employed RNAi-mediated strategies (Perrimon et al., 2010) using the GMR driver. First, we validated RNAi by RT/PCR and observed that mRNA corresponding to Pkc53E-B is greatly reduced to about 19 % of wild-type [from 45.3 $\pm$ 8.5 (n = 3) to 8.9 $\pm$ 5.1 (n = 3)] (Lanes 5, 9, Figure 2A). We also performed eye-PKC-RNAi, which was validated by Western blotting with a great reduction of eye-PKC to 4.9 $\pm$ 3.4% (n = 4) of wild-type (Figure S1). Subsequently, we investigated the retinal morphology by fluorescence microscopy using GFP tagged arrestin 2 (Arr2-GFP) (Kristaponyte et al., 2012) as the reporter.

We show eye-PKC-RNAi led to more severe degeneration affecting mostly size initially with less impact on the number, orientation, and arrangement of rhabdomeres within the cluster (Figure 2B). In contrast, Pkc53E-RNAi resulted in an age-dependent retinal degeneration characterized by distorted ommatidia clusters with missing rhabdomere (Figure 2B). Indeed, in 8-day old retinas, most ommatidia clusters lack about two rhabdomeres with 4.8 $\pm$ 0.7 (n = 3) remained. In contrast, overexpression of the B-isoform of Pkc53E, which increases the mRNA content about two-fold (203.5 $\pm$17.2%, n = 3) (Figure 2A), did not significantly modify the retinal morphology (Figure 2C, D; Figure 8A). Together, we demonstrate that both Pkc53E and eye-PKC are involved in the regulation of the rhabdomere integrity, reducing the expression of each kinase leads to distinct phenotypes.

Conventional PKC has been implicated in regulating the actin cytoskeleton. Therefore, we examined how the actin-based rhabdomeres might be affected using Actin-GFP as the reporter (Roper et al., 2005; Shieh et al., 2021). Indeed, Pkc53E-RNAi results in missing rhabdomeres, which is accompanied by the abnormal arrangement of ommatidia clusters (Figure 2B). We show that the number of rhabdomeres is reduced from seven to about five in

10-day old retinas, which is similar to that observed using Arr2-GFP. In contrast, eye-PKC-RNAi initially affects the rhabdomere diameter, but not the rhabdomere number (Figure 2B). The age-dependent reduction of rhabdomere number (Figure 2C) or area (Figure 2D) upon knockdown or overexpression of Pkc53E was compared.

Together, our findings strongly support that a reduction of the Pkc53E activity directly or indirectly affects the actin cytoskeleton of rhabdomeres. We thus propose that Pkc53E regulates processes to promote the stability of rhabdomeres.

Downregulation of either Pkc53E, or eye-PKC by RNAi enhanced the degeneration of *norpA*^{P24} photoreceptors

We explored whether Pkc53E is operating in the visual cascade downstream of NorpA, similar to eye-PKC. We speculate that both PKC's would not be active in *norpA*^{P24} photoreceptors lacking NorpA/PLCβ4. Consequently, downregulation of each PKC would not modify the phenotype caused by the loss of NorpA. Unexpectedly, we observed that Pkc53E-RNAi greatly exacerbated retinal degeneration of *norpA*^{P24} photoreceptors (Figure 3 A, C). Similarly, eye-PKC-RNAi also showed a similar but less severe effect (Figure 3 A, C). Taken together, we conclude that both eye-PKC and Pkc53E remain active in mutants missing PLCβ4, indicating alternate activation by another PLCβ.

Plc21C-RNAi enhanced the degeneration of *norpA*^{P24} photoreceptors

We investigated the contribution of phospholipase C at 21C (Plc21C), which is known to couple to Gq in *norpA*^{P24} photoreceptors (Ogueta et al., 2018). Plc21C functions in olfaction (Kain et al., 2008) and also has been shown to participate in the light-dependent regulation of the circadian clock (Ogueta et al., 2018). We speculate if Plc21C promotes the activation of two cPKC's, downregulation of Plc21C would exacerbate retinal degeneration of *norpA*^{P24} photoreceptors. Indeed, we observed that retinal degeneration was greatly accelerated by Plc21C-RNAi, as evident in 7-day old flies (Figure 3B, D). However, Plc21C-RNAi did not modify the retinal morphology in wild-type genetic background (Figure 3B, D), indicating that it is not involved in the maintenance of rhabdomeres.

Quantitative PCR analyses indicated that mRNA for Plc21C was reduced by 41 $\pm$ 11% (n = 3) in the fly head following RNAi-mediated downregulation.

Taken together, our findings support the role of Plc21C, a second PLCβ in the eye, which can be activated in the absence of NorpA leading to the activation of Pkc53E and eye-PKC.

Gαq-RNAi leads to retinal degeneration, which is not modified by Pkc53E-RNAi

We explored how Plc21C might be activated in *norpA*^{P24} photoreceptors. Like PLCβ4, activation of Plc21C also involves the heterotrimeric Gq protein (Kain et al., 2008). We first investigated the role of Gαq via RNAi employing a modified Rh1 containing a mCherry tag as the reporter. We show Rh1-mCherry is present in the rhabdomere of R1-6 photoreceptors in wild-type (Figure 4A) whereas Gαq-RNAi leads to accumulation of internalized Rh1-mCherry and retinal degeneration as shown in 5-d old retinas (Figure 4B). This phenotype is similar to that observed in *norpA*^{P24} (Figure 4 D), consistent with the notion that a reduced NorpA or Gαq activity greatly diminishes the Ca^{2+} influx critical for the recycling of the internalized rhodopsin.

We investigated whether Gαq coupled to Plc21C leading to the activation of Pkc53E in *norpA*^{P24} photoreceptors. As shown before, retinal degeneration in *norpA*^{P24} photoreceptors was enhanced by Pkc53E-RNAi (Figure 4D, F). In contrast, degeneration caused by Gαq-RNAi was not further modified by Pkc53E-RNAi (Figure 4B, C), suggesting that Pkc53E is not active when Gq is greatly reduced. Similarly, eye-PKC RNAi did not modify retinal degeneration by Gαq-RNAi (not shown). Taken together, Gq is likely to couple to Plc21C leading to the activation of both PKC's when NorpA is missing.

Molecular characterization of *Drosophila* adducin

Members of the cPKC family have been implicated in remodeling of the actin cytoskeleton (Larsson, 2006). We explored whether Pkc53E regulates adducin, a cytoskeletal protein critical for the assembly of the membrane skeleton by regulating the interaction between the actin filament and the spectrin network (Matsuoka et al., 2000). In vertebrates, there are three adducin homologs, α-adducin (ADD1), β-adducin (ADD2), and γ-adducin (ADD3).

Functional adducin consists of heterotetramers that are made up of either αβ or αγ heterodimer (Matsuoka et al., 2000).

Drosophila contains one adducin gene, *hts* (Yue and Spradling, 1992) that generates three adducin-like polypeptides of 739 (Add1 or isoforms Q, R), 718 (Add2 or isoforms I, L, M), and 716 aa (Add3 or isoforms O, S) with different C-terminal sequences (Figure 5B). We show, for the first time, that mRNA transcripts corresponding to these three isoforms are expressed in photoreceptors (Figure 5C). Like mammalian isoforms, *Drosophila* adducin contains a globular domain at the N-terminus, a neck domain, and a C-terminal tail with the MARCKS-like domain that contains the conserved PKC phosphorylation sites (Figure 5A, B).

We investigated the expression of adducin isoforms in photoreceptors by Western blotting using a monoclonal antibody (1B1) that recognizes its N-terminal sequence. We observed multiple protein bands including two prominent bands above 80 kD in size (Figure 5D), which may correspond to Add1 (739 aa, upper band), and Add2/Add3 (718/716 aa, lower band), respectively. Significantly, these protein isoforms appear ubiquitously expressed as they are present in head extracts from both wild-type and *glass* mutants (Figure 5D).

Reduced phosphorylation of adducin at $Ser^{726/705/703}$ in a *Pkc53E* null allele

To explore whether Pkc53E phosphorylates adducin at the conserved PKC site, $Ser^{726/705/703}$, in each isoform, *in vivo*, we employed Western blotting using polyclonal antibodies that recognize phosphorylated $Ser^{726/705/703}$. Indeed, we observed that both upper and lower bands of adducin were phosphorylated in wild-type retinal extracts (Figure 5E). We calculated the steady-state level of total phosphorylated adducin, and demonstrate that phosphorylated adducin was reduced by 57.5 % $\pm$ 5.2% (n = 3) in $pkc53E^{\Delta 28}$, but was not significantly affected in $inaC^{P209}$ (Figure 5E, F). Together, our findings strongly support that phosphorylation of adducin is partly regulated by Pkc53E *in vivo*.

Hts-RNAi leads to loss of rhabdomeres or ommatidial clusters similar to Pkc53E-RNAi

We explored the function of adducin in photoreceptors via RNAi-mediated strategies. First, we validated Hts-RNAi using Western blotting. Because adducin is ubiquitously expressed, the level of adducin in the fly head was not greatly reduced by Hts-RNAi (Figure 6A). Therefore, we chose a transgenic fly that co-expressed a mCherry tagged adducin (Add2) that served as a marker for Hts-RNAi (Figure 6A). Indeed, we demonstrate that the expression of the tagged adducin was greatly reduced by Hts-RNAi by Western blotting (Figure 6A).

Using Actin-GFP as a reporter, we show that Hts-RNAi led to a loss of rhabdomeres and occasionally, missing ommatidia clusters, in 7-day old flies (Figure 6B). This defect is further exacerbated and a loss of rhabdomeres was observed in 14-day flies. This phenotype of Hts-RNAi is similar to that observed in Pkc53E-RNAi. Importantly, downregulation of both adducin and Pkc53E by RNAi results in a phenotype similar to that of Hts-RNA, suggesting that adducin is likely a downstream target of Pkc53E involved in the maintenance of the actin cytoskeleton in photoreceptors.

Overexpression of a tagged adducin leads to apical expansion of rhabdomeres

To further explore the role of adducin, we overexpressed a modified adducin (Add2) that contains a C-terminal mCherry tag using the GMR driver. Interestingly, overexpression led to sporadic 'apical expansion' characterized by the overgrowth of the actin-based cytoskeleton in the rhabdomere (Figure 7A). Importantly, this abnormal expansion of the actin cytoskeleton occurs in all rhabdomeres within the same ommatidia, in which the diameter of rhabdomere increases about 2.73 ± 0.31 ($n = 5$) fold, compared to that of wild-type. Furthermore, the expansion affects the patterning of rhabdomere clusters as the typical trapezoidal arrangement of R1-6 rhabdomeres becomes less evident (Figure 7 A, right panel). The expansion phenotype is dependent on the copy number of the transgene; one copy resulted in expansion in $32.3 \pm 13.5\%$ ($n = 10$) while two copies gave rise to $46.1 \pm 3.3\%$ ($n = 6$) of ommatidia clusters with abnormally enlarged rhabdomeres. Despite the expansion, the external appearance of the compound eye is not significantly altered (not shown).

The presence of these expanded rhabdomeres also led to a distorted dpp (deep pseudopupil) from either Actin-GFP or Rh1-mCherry (Figure 7A) as the alignment of the optical axis within the compound eye is affected (Figure 7A, middle, lower panels). The expansion phenotype is detected in late pupal photoreceptors, indicating that

it occurs during the morphogenesis of rhabdomere following the differentiation of photoreceptors. We propose that adducin is critically involved in the regulation of rhabdomere expansion in pupal photoreceptors. These enlarged rhabdomeres may be caused by the dominant-negative effect of the tagged adducin unable to cap the growing end of the actin filament and/or to recruit β-spectrin that is critical for regulating the membrane domain (see below).

β-Spectrin-RNAi also leads to apical expansion of ommatidia

We explored the cause of the expansion of the actin cytoskeleton by comparing the phenotype to that from the knockdown of several known components involved in the actin-spectrin network including α-spectrin, β-spectrin, β_H-spectrin (karst), and ankyrin1. Indeed, knockdown of either α- or β-spectrin also led to expansion similar to that observed in the overexpression of tagged Add2 (Figure 7B). Specifically, β-spectrin-RNAi resulted in the apical expansion of the ommatidia cluster with a frequency, 15.1$\pm$ 2.1% (n = 7), which is about half of those observed in flies expressing the tagged Add2. In contrast, α-spectrin-RNAi also led to enlarged rhabdomeres with reduced numbers of ommatidia clusters while β_H-spectrin/karst-RNAi also exhibits abnormal rhabdomere organization within clusters. Based on the findings, we propose that the overexpression of the tagged Add2 negatively affects the formation of the actin-spectrin network that is critical for delineation between the apical and basolateral domains in pupal photoreceptors.

Apically expanded rhabdomeres are affected by Pkc53E-RNAi

To further explore the relationship between adducin and Pkc53E in pupal photoreceptors, we investigated how changes of Pkc53E activity would modify the actin cytoskeleton of those abnormal rhabdomeres. Importantly, we show that neither RNAi nor overexpression of Pkc53E-B affects the relative abundance of apically expanded rhabdomeres (Figure 8A), strongly suggesting that Pkc53E is not involved in the regulation of adducin in pupal photoreceptors. In contrast, Pkc53E-RNAi accelerates retinal degeneration of those enlarged rhabdomeres in adult photoreceptors leading to distorted ommatidia as rhabdomeres become flatten or elongated (Figure 8A, B). In contrast, overexpression of the B isoform of Pkc53E did not affect the retinal morphology nor accelerated

degeneration of flies expressing tagged Add2 (Figure 8A, B). Taken together, we conclude that Pkc53E is likely to regulate adducin to affect the actin cytoskeleton in adult photoreceptors.

Discussion

Here we uncovered the role of a photoreceptor-specific isoform of Pkc53E, Pkc53E-B, in the maintenance of the actin cytoskeleton of rhabdomeres in *Drosophila*. We demonstrate that Pkc53E-B is activated downstream of NorpA in the visual cascade. However, when NorpA is absent, Plc21C (Shortridge et al., 1991) can be activated by Gq to switch on Pkc53E. We explored whether Pkc53E regulates adducin, a cytoskeletal protein critical for the assembly of the membrane skeleton (Baines, 2010). Adducin regulates the linkage between actin filaments and the spectrin network, which is negatively affected by PKC phosphorylation (Barkalow et al., 2003; Matsuoka et al., 1998; Matsuoka et al., 2000). Indeed, in a null allele of *pkc53E*, we observed a reduced level of phosphorylated adducin. Furthermore, Hts-RNAi resulted in missing rhabdomeres, which is more severe than Pkc53E-RNAi, suggesting that Pkc53E regulates adducin in adult photoreceptors. Interestingly, overexpression of a mCherry tagged adducin leads to the apical expansion of rhabdomeres, which is also observed in β-spectrin-RNAi. We speculate that the expansion phenotype is caused by the interference of the actin-spectrin interaction that may impact the apical-basal patterning of pupal photoreceptors. Importantly, Pkc53E is not involved in regulating adducin during pupal development.

Thus, in adult photoreceptors a rise of intracellular Ca^{2+} and the release of DAG accompanying the activation of PLCβ4 elevates the Pkc53E activity: Pkc53E phosphorylates adducin and releases it from the actin filament and the spectrin complex. To re-establish the link with the actin-spectrin network, phosphorylated adducin may undergo dephosphorylation by cytosolic protein phosphatases. The dynamic regulation of Pkc53E by light serves to fine-tune the linkage between the spectrin-based membrane skeleton and the plasma membrane, which also is critical for processes including endocytosis and trafficking of transmembrane proteins.

<u>Pkc53E-B is a photoreceptor-specific isoform that regulates the actin cytoskeleton of rhabdomeres</u>

Visual signaling leads to the activation of Pkc53E and eye-PKC. While eye-PKC is tethered to the multimeric protein complex (Adamski et al., 1998; Popescu et al., 2006; Tsunoda and Zuker, 1999) and is involved in fast activation and deactivation of the visual response (Hardie et al., 1993; Ranganathan et al., 1991; Smith et al., 1991) (Figure 9), little is known regarding the role of Pkc53E in the eye. The Pkc53E gene gives rise to four protein isoforms

with different C1 domains (Flybase). We established that mRNA coding for the B-isoform of Pkc53E is highly expressed in photoreceptors. Consistently, Pkc53E-B mRNA is drastically reduced by Pkc53E-RNAi using the photoreceptor-specific GMR driver. Pkc53E-B is the longest protein isoform consisting of 679 aa that displays 57% sequence similarities to eye-PKC. We demonstrate, for the first time, that loss of function of *pkc53E* leads to retinal degeneration. Moreover, downregulation of Pkc53E-B results in a loss of rhabdomeres while overexpression of *pkc53E-B* exerts a little effect.

Pkc53E-B is likely acting downstream of NorpA/PLCβ4. However, we discovered that both Pkc53E and eye-PKC are partially active in *norpA* photoreceptors, and demonstrate an alternative mechanism in which Plc21C is deployed leading to the activation of two PKC's (Figure 9). A lack of NorpA likely leads to unregulated Gq, as NorpA serves as GTPase activating protein for inactivating Gq (Cook et al., 2000). The prolonged Gq activity thus may promote its coupling to Plc21C.

Phosphorylation and function of adducin in photoreceptors

The *Drosophila* adducin gene, *hts*, was originally identified for its role in the ring canal formation of the oocyte (Yue and Spradling, 1992). The *hts* locus encodes at least eight polypeptides including three adducin-like proteins containing the MARCKS-related domain (Flybase). These three isoforms vary in their C-terminal sequences and may correspond to the three mammalian homologs (Citterio et al., 1999; Joshi et al., 1991). Previously, a doublet of adducin-like polypeptides was observed in the Western blot (Pielage et al., 2011; Wang et al., 2014). Here we show that the adducin doublet is likely to encompass three related polypeptides. All adducin isoforms appear phosphorylated in photoreceptors, and levels of phosphorylated adducin are greatly reduced in a null allele of *pkc53E*, suggesting that Pkc53E is critical for the phosphorylation of adducin. Moreover, Hts-RNAi results in a severe loss of rhabdomeres, which is not modified by Pkc53E-RNAi, supporting Pkc53E regulates adducin *in vivo*.

We overexpressed a mCherry tagged Add2 in photoreceptors and observed the apical expansion characterized by the overgrowth of the actin cytoskeleton of the rhabdomere in about 32% of ommatidia clusters. This expansion phenotype is similar to that observed in β-spectrin-RNAi, suggesting that expression of the modified adducin

interferes with the formation of the spectrin network. The mCherry tag at the C-terminus of adducin may impact the activity of the MARCKS-related domain that is critically involved in the interaction with the spectrin network.

Spectrins (α-spectrin, β-spectrin, and β_H-spectrin) form oligomers that are the basis of the spectrin-based membrane skeleton, which localizes in the cytoplasmic side of the plasma membrane (Bennett and Baines, 2001). Specifically, α/β_H-spectrins are localized at the apical domain (Pellikka et al., 2002) while α/β-spectrins in the basolateral domain of photoreceptors (Chen et al., 2009). It has been shown that removal of either α- or β-spectrin leads to the expanded apical domain while overexpression of β-spectrin reduces it (Chen et al., 2009), suggesting that basolaterally localized α/β-spectrins are critical for the maintenance of the apical domain possibly by regulating the polarity cues. Moreover, spectrins may regulate cell shape by controlling the Hippo signaling (Deng et al., 2020; Fletcher et al., 2015) to affect tissue size. How each mechanism contributes to the rhabdomere expansion remains to be explored.

While adducin was first identified for its role in the assembly of the spectrin-based membrane cytoskeleton in erythrocytes (Matsuoka et al., 2000), it appears to exert diverse functions. In epithelia, adducin is critical for cell-cell adhesion (Abdi and Bennett, 2008), regulating cell junctions and permeability (Naydenov and Ivanov, 2011). Interestingly, adducin was shown to be localized in the nucleus of cultured cells that were not forming contact with neighboring cells (Chen et al., 2011). In the nervous system, adducin is involved in the assembly of synapses by orchestrating the remodeling of dendritic spins (Bednarek and Caroni, 2011; Engmann et al., 2016); loss of β-adducin reduces spin formation affecting synaptic plasticity (Rabenstein et al., 2005).

To sum up, adducin regulates the interaction between actin filaments and the spectrin network. Here we demonstrate two distinct functions of adducin in *Drosophila*. In adult photoreceptors, adducin is involved in the maintenance of the actin cytoskeleton supporting the rhabdomere, which is regulated by Pkc53E. In contrast, adducin is critical for rhabdomere morphogenesis during pupal development, which is not affected by changes in the Pkc53E activity.

Hts-RNAi and a dominant-negative of adducin lead to two distinct phenotypes

In erythrocytes, the functions of adducin include (1) capping the growing end of the actin filament, (2) linking actin filaments to the spectrin network, and (3) bundling actin filaments (Matsuoka et al., 2000). We employed two different strategies to investigate the role of adducin in *Drosophila*. We show that Hts-RNAi led to a loss of rhabdomeres in adult photoreceptors. In contrast, overexpression of a tagged Add2, which appears to act in a dominant-negative manner, primarily affects rhabdomere morphogenesis during pupal development. We speculate that adducin is stable and therefore is not greatly affected by RNAi during development. However, the co-expression of the tagged Add2 when incorporated into adducin oligomers appears to prominently interfere with the interaction with the spectrin network. It is likely that the inclusion of the mCherry tag at the carboxyl terminus of adducin negatively impacts its association with actin filaments.

A hypothetical model linking activation of Pkc53E to the reorganization of the actin cytoskeleton

In summary, we show that Pkc53E plays a role in regulating the stability of the actin cytoskeleton. Pkc53E probably phosphorylates adducin that controls the linkage between actin filaments and the spectrin network. Thus, transmembrane signaling that activates PLCβ or PLCγ leading to the activation of cPKC may transiently uncouple the spectrin network from actin filaments. This triggers the extension of actin filaments and promotes the remodeling of the actin cytoskeleton, which is critical for maintaining the cell shape and possibly for regulating protein turnover in the plasma membrane. Remodeling of the membrane cytoskeleton may facilitate endocytosis and trafficking of transmembrane proteins, which fine-tune the signaling event. In the visual signaling in which activation of rhodopsin leads to an increase of cytosolic Ca^{2+} and transient activation of cPKC. Both Ca^{2+} and cPKC are involved in the stability of the actin cytoskeleton (Figure 9). Indeed, when the canonical pathway to turn on cPKC is missing, an alternate pathway that uses Plc21C is deployed to supports the maintenance of *Drosophila* photoreceptors. We propose that regulation of the actin cytoskeleton is a fundamental event for the PLC-mediated signaling mechanisms.

Figure legends

Figure 1: Characterization of a *pkc53E* null allele and identification of a photoreceptor-specific Pkc53E isoform

A, Loss of function in *pkc53E* leads to retinal degeneration. Shown is a Western blot containing extracts from wild-type, $pkc53E^{\Delta 28}$, and $inaC^{P209}$ (seven-day-old) probed with antibodies against Rh1, fascin (loading control), and adducin/Hts, respectively. Protein standards are indicated on the right. **B**, A graphic map depicting the coding sequences (filled boxes) of six alternatively spliced *pkc53E* transcripts, A-F. **C**, Alignment of the N-terminal sequences from the six Pkc53E isoforms. All isoforms have two distinct C1/DAG binding domains (arrows, 45-110 aa; 120-173 aa in isoform B), except the D isoform. Amino acid identities are boxed. **D**, Identification of the photoreceptor-specific isoform by RT/PCR. Shown are PCR products analyzed by polyacrylamide gel (8%). Even-numbered lanes represent PCR products from wild-type and odd-numbered lanes, *glass* mutants. Rp49 serves as a positive control whereas Arr1, a positive control for wild-type and negative control for *glass* for its expression in photoreceptors. DNA fragments corresponding to the predicted PCR products are marked with asterisks (*) in wild-type lanes. The B isoform of Pkc53E appears highly expressed in photoreceptors as it is drastically reduced in the *glass* mutant (lanes 9). DNA size standards are shown on the right.

Figure 2: Downregulation of Pkc53E or eye-PKC in photoreceptors leads to distinct degeneration phenotype

A, Validation of RNAi and overexpression of *pkc53E* by RT/PCR. The mRNA level for the B-isoform of Pkc53E (*) is drastically reduced to 8.9 $\pm$ 5.1 (n = 3) when compared to the control of 45.3 $\pm$ 8.5 (n = 3, lanes 5, 9). In contrast, overexpression of *pkc53E-B* leads to about a two-fold increase of the mRNA (lanes 8, 12). Oligonucleotide primer sets used are indicated below and the first-strand cDNA templates from Pkc53E-RNAi (lanes 1, 5, and 9), wild-type (2, 6, and 10), flies expressing GMR driver alone (3, 7, and 11), and *pkc53E* overexpressing flies (4, 8, and 12), respectively, were used. The PCR products corresponding to the B-isoform are marked with asterisks on the left in the wild-type lanes. **B**, Retinal degeneration caused by Pkc53E-RNAi or eye-PKC-RNAi using Arr2-GFP (left) or Actin-GFP (right) as the reporter. Arr2-GFP was engineered to be expressed in R1-6 photoreceptors whereas Actin-GFP was targeted to all photoreceptors (R1-R8) driven by the GMR driver. Shown are representative images of 8-

day old flies. Scale bars on the left panel, 5 μm, and on the right panel, 2 μm. **C**, The age-dependent loss of rhabdomeres in the *pkc* (Pkc53E RNAi, Pkc53E overexpression, eye-PKC RNAi) mutants using Actin-GFP as the reporter. Each time point represents the mean of three flies (mean ± S.E.M, n = 3). **D**, The age-dependent changes of rhabdomere area in various *pkc* mutant backgrounds. Shown are mean ± S.E.M (n = 3) from three independent experiments.

Figure 3: Activation of Plc21C when NorpA/PLCβ4 is absent

A, Retinal degeneration of $norpA^{P24}$ is enhanced by either Pkc53E-RNAi or eye-PKC-RNAi. Shown are retinal morphology in 7-day old flies in either wild-type (left panel) or $norpA^{P24}$ (right) genetic background. Arr2-GFP was used as the reporter. Scale bars, 2 μm. **B**, Degeneration of $norpA^{P24}$ photoreceptors is enhanced by Plc21C-RNAi. In contrast, Plc21C-RNAi alone did not affect retinal morphology in wild-type backgrounds. Shown are retinas of 7-day old flies. Scale bars, 5 μm. **C**, **D**, Rhabdomere areas (in arbitrary units, n = 4) were quantified and shown in a histogram.

Figure 4: Pkc53E-RNAi does not modify degeneration caused by Gαq-RNAi

Gαq-RNAi leads to retinal degeneration that is accompanied by the accumulation of internalized Rh1 rhodopsin (**B**), similar to $norpA^{P24}$ (**D**) when compared to wild-type (**A**). Rh1-mCherry was used as the reporter. Internalized Rh1-mCherry are present in large vesicles surrounding the rhabdomere and some are marked with arrows. Retinal degeneration of Gαq-RNAi is not enhanced by Pkc53E-RNAi (**C**), unlike degeneration of $norpA^{P24}$ (**F**). Shown are retinas of 6-day old flies. Scale bars, 5 μm

Figure 5: Expression of adducin-like isoforms of Hts and phosphorylation by Pkc53E

A, A graphic representation of the domain structure in three *Drosophila* adducin isoforms that consist of 739 (Add1), 718 (Add2), or 716 aa (Add3), respectively. All isoforms contain a globular head domain, a neck domain, and the variable C-terminal tail sequence with the MARCKS-related domain. **B**, The alignment of the C-terminal sequences

that contain part of the tail domain. Amino acid sequence identities are boxed and the conserved PKC phosphorylation sites at $Ser^{726/705/703}$ are highlighted in red. **C**, Expression of three adducin isoforms by RT/PCR. Sequence-specific primers (see Materials and Methods) were used for each isoform. The predicted PCR product is indicated on the right. DNA molecular weight standards are shown on the left. **D**, Western blot analysis of wild-type and *glass* head extracts using monoclonal antibodies for Hts (1B1), TRP, and actin, respectively. Both wild-type and *glass* head extracts contain Hts including two strong bands that may correspond to 739 aa (Add1) and 718/716 aa (Add2/Add3) isoforms. **E**, Phosphorylation of adducin at the conserved PKC site, $Ser^{726/705/703}$ in each isoform. Shown are Western blots probed with either 1B1 (right panel) or polyclonal antibodies for phospho-$Ser^{726/705/703}$ (left). Both adducin bands encompassing all isoforms were phosphorylated *in vivo*, and phosphorylation was greatly reduced in $Pkc53E^{\Delta 28}$, but not in $inaC^{P209}$. Total and phosphorylated adducin were quantified using fascin as a loading control. Levels of phosphorylated adducin in the mutants were compared in a histogram (**F**). Each lane contained protein extracts prepared from four retinas.

Figure 6: Hts-RNAi leads to a more severe retinal degeneration than Pkc53E-RNAi

A, Validation of Hts-RNAi by the loss of tagged Add2 expression via Western blotting. The mCherry tagged Add2 with an estimated size of 115 kD migrates above the endogenous adducin in SDS/PAGE (10%). Protein size markers are indicated on the left. **B**, Retinal morphology of Hts-RNAi using Actin-GFP as the marker. Hts-RNAi exhibits a phenotype with loss of rhabdomeres, which is more severe than that of Pkc53E-RNAi. Pkc53E-RNAi did not modify the retinal morphology by Hts-RNAi. Shown are retinas of 7-day old flies. Scale bars, 5 μm

Figure 7: Overexpression of adducin leads to apical expansion of the actin cytoskeleton similar to β-spectrin-RNAi

A, Overexpression of mCherry tagged adducin, Add2, led to the apical expansion of rhabdomeres. In the compound eye, about 32.3 $\pm$ 13.5% (n = 10) of ommatidia clusters (right panel, top) contain enlarged rhabdomeres that seem to project further outward when compared to control (left panel, top). The diameter of rhabdomere is increased to 2.73

± 0.31 (n = 5) fold. The dpp becomes less distinct as visualized either by Actin-GFP (middle) or Rh1-mCherry (bottom), compared to wild-type (left panel). **B**, Spectrin-RNAi also leads to apical expansion. α-spectrin-RNAi (right panel, top) results in an enlarged actin cytoskeleton in all rhabdomeres. In contrast, β-spectrin-RNAi display enlarged rhabdomeres with reduced frequency compared to the expression of tagged adducin. β_H-spectrin/karst-RNAi (right panel) also leads to apical expansion accompanied by the abnormal arrangement of rhabdomeres. In contrast, ankyrin1-RNAi has no significant effect on retinal morphology. Scale bars in **A**, 5 μm (top panel), 20 μm (bottom panels), and in **B**, 2 μm.

Figure 8: The expanded actin cytoskeleton is negatively affected by Pkc-53E-RNAi

A, Modulation of the apical expansion phenotype by Pkc53E. Effects of RNAi or overexpression of Pkc53E-B in wild-type (left panel) and the Add2-mCherry overexpressing background (right panel) using Actin-GFP as the reporter. In the Add2-mCherry background, downregulation of Pkc53E resulted in degeneration of the abnormally expanded rhabdomeres (middle panel) while overexpression did not significantly modify the actin cytoskeleton of rhabdomeres (bottom panel). **B**, Higher magnification (1000X) of the expanded rhabdomeres with different Pkc53E activity. The abnormally enlarged rhabdomeres became distorted or flattened in adult photoreceptors (middle panel) when pKC53E is downregulated by RNAi. Scale bars 5 μm in **A** and 2 μm in **B**.

Figure 9: Role of Pkc53E to regulate adducin to promote the maintenance of the actin cytoskeleton

In wild-type photoreceptors (left panel), light activates rhodopsin (Rh1) that couples to Gq leading to the activation of PLCβ4 /NorpA. PLCβ4 generates DAG and increases Ca^{2+} leading to the activation of eye-PKC and Pkc53E. Eye-PKC phosphorylates the TRP Ca^{2+} channel to promote fast deactivation of the visual response. In contrast, Pkc53E phosphorylates adducin (Add) to orchestrate the remodeling of the actin cytoskeleton by uncoupling the interaction between actin filaments and the spectrin network. In *norpA*^{P24} photoreceptors (right panel), Plc21C is activated instead of PLCβ4 leading to the activation of eye-PKC and Pkc53E.

References

Abdi, K.M., and V. Bennett. 2008. Adducin promotes micrometer-scale organization of beta2-spectrin in lateral membranes of bronchial epithelial cells. *Mol Biol Cell*. 19:536-545.

Adamski, F.M., M.Y. Zhu, F. Bahiraei, and B.H. Shieh. 1998. Interaction of eye protein kinase C and INAD in Drosophila. Localization of binding domains and electrophysiological characterization of a loss of association in transgenic flies. *J Biol Chem*. 273:17713-17719.

Baines, A.J. 2010. The spectrin-ankyrin-4.1-adducin membrane skeleton: adapting eukaryotic cells to the demands of animal life. *Protoplasma*. 244:99-131.

Barkalow, K.L., J.E. Italiano, Jr., D.E. Chou, Y. Matsuoka, V. Bennett, and J.H. Hartwig. 2003. Alpha-adducin dissociates from F-actin and spectrin during platelet activation. *J Cell Biol*. 161:557-570.

Bednarek, E., and P. Caroni. 2011. beta-Adducin is required for stable assembly of new synapses and improved memory upon environmental enrichment. *Neuron*. 69:1132-1146.

Bennett, V., and A.J. Baines. 2001. Spectrin and ankyrin-based pathways: metazoan inventions for integrating cells into tissues. *Physiol Rev*. 81:1353-1392.

Cerny, A.C., T. Oberacker, J. Pfannstiel, S. Weigold, C. Will, and A. Huber. 2013. Mutation of light-dependent phosphorylation sites of the Drosophila transient receptor potential-like (TRPL) ion channel affects its subcellular localization and stability. *J Biol Chem*. 288:15600-15613.

Chen, C.L., Y.P. Lin, Y.C. Lai, and H.C. Chen. 2011. alpha-Adducin translocates to the nucleus upon loss of cell-cell adhesions. *Traffic*. 12:1327-1340.

Chen, T.W., G. Chen, L.J. Funkhouser, and S.C. Nam. 2009. Membrane domain modulation by Spectrins in Drosophila photoreceptor morphogenesis. *Genesis*. 47:744-750.

Chirgwin, J.M., A.E. Przybyla, R.J. MacDonald, and W.J. Rutter. 1979. Isolation of biologically active ribonucleic acid from sources enriched in ribonuclease. *Biochemistry*. 18:5294-5299.

Citterio, L., T. Azzani, S. Duga, and G. Bianchi. 1999. Genomic organization of the human gamma adducin gene. *Biochem Biophys Res Commun*. 266:110-114.

Cook, B., M. Bar-Yaacov, H. Cohen Ben-Ami, R.E. Goldstein, Z. Paroush, Z. Selinger, and B. Minke. 2000. Phospholipase C and termination of G-protein-mediated signalling in vivo. *Nat Cell Biol*. 2:296-301.

Deng, H., L. Yang, P. Wen, H. Lei, P. Blount, and D. Pan. 2020. Spectrin couples cell shape, cortical tension, and Hippo signaling in retinal epithelial morphogenesis. *J Cell Biol*. 219.

Engmann, O., A. Giralt, and J.A. Girault. 2016. Acute drug-induced spine changes in the nucleus accumbens are dependent on beta-adducin. *Neuropharmacology*. 110:333-342.

Fletcher, G.C., A. Elbediwy, I. Khanal, P.S. Ribeiro, N. Tapon, and B.J. Thompson. 2015. The Spectrin cytoskeleton regulates the Hippo signalling pathway. *EMBO J*. 34:940-954.

Hardie, R.C., and M. Juusola. 2015. Phototransduction in Drosophila. *Curr Opin Neurobiol*. 34:37-45.

Hardie, R.C., A. Peretz, E. Suss-Toby, A. Rom-Glas, S.A. Bishop, Z. Selinger, and B. Minke. 1993. Protein kinase C is required for light adaptation in Drosophila photoreceptors. *Nature*. 363:634-637.

Hu, Y., R. Sopko, M. Foos, C. Kelley, I. Flockhart, N. Ammeux, X. Wang, L. Perkins, N. Perrimon, and S.E. Mohr. 2013. FlyPrimerBank: an online database for Drosophila melanogaster gene expression analysis and knockdown evaluation of RNAi reagents. *G3 (Bethesda)*. 3:1607-1616.

Joshi, R., D.M. Gilligan, E. Otto, T. McLaughlin, and V. Bennett. 1991. Primary structure and domain organization of human alpha and beta adducin. *J Cell Biol*. 115:665-675.

Kain, P., T.S. Chakraborty, S. Sundaram, O. Siddiqi, V. Rodrigues, and G. Hasan. 2008. Reduced odor responses from antennal neurons of G(q)alpha, phospholipase Cbeta, and rdgA mutants in Drosophila support a role for a phospholipid intermediate in insect olfactory transduction. *The Journal of neuroscience : the official journal of the Society for Neuroscience*. 28:4745-4755.

Kristaponyte, I., Y. Hong, H. Lu, and B.H. Shieh. 2012. Role of rhodopsin and arrestin phosphorylation in retinal degeneration of Drosophila. *The Journal of neuroscience : the official journal of the Society for Neuroscience*. 32:10758-10766.

Larsson, C. 2006. Protein kinase C and the regulation of the actin cytoskeleton. *Cell Signal*. 18:276-284.
Lipp, P., and G. Reither. 2011. Protein kinase C: the "masters" of calcium and lipid. *Cold Spring Harb Perspect Biol*. 3.
Matsuoka, Y., X. Li, and V. Bennett. 1998. Adducin is an in vivo substrate for protein kinase C: phosphorylation in the MARCKS-related domain inhibits activity in promoting spectrin-actin complexes and occurs in many cells, including dendritic spines of neurons. *J Cell Biol*. 142:485-497.
Matsuoka, Y., X. Li, and V. Bennett. 2000. Adducin: structure, function and regulation. *Cell Mol Life Sci*. 57:884-895.
Montell, C. 2012. Drosophila visual transduction. *Trends Neurosci*. 35:356-363.
Moses, K., M.C. Ellis, and G.M. Rubin. 1989. The glass gene encodes a zinc-finger protein required by Drosophila photoreceptor cells. *Nature*. 340:531-536.
Naydenov, N.G., and A.I. Ivanov. 2011. Spectrin-adducin membrane skeleton: A missing link between epithelial junctions and the actin cytoskeletion? *Bioarchitecture*. 1:186-191.
Ogueta, M., R.C. Hardie, and R. Stanewsky. 2018. Non-canonical Phototransduction Mediates Synchronization of the Drosophila melanogaster Circadian Clock and Retinal Light Responses. *Curr Biol*. 28:1725-1735 e1723.
Pellikka, M., G. Tanentzapf, M. Pinto, C. Smith, C.J. McGlade, D.F. Ready, and U. Tepass. 2002. Crumbs, the Drosophila homologue of human CRB1/RP12, is essential for photoreceptor morphogenesis. *Nature*. 416:143-149.
Peng, L., D.C. Popescu, N. Wang, and B.H. Shieh. 2008. Anchoring TRP to the INAD macromolecular complex requires the last 14 residues in its carboxyl terminus. *J Neurochem*. 104:1526-1535.
Perrimon, N., J.Q. Ni, and L. Perkins. 2010. In vivo RNAi: today and tomorrow. *Cold Spring Harb Perspect Biol*. 2:a003640.
Pielage, J., V. Bulat, J.B. Zuchero, R.D. Fetter, and G.W. Davis. 2011. Hts/Adducin controls synaptic elaboration and elimination. *Neuron*. 69:1114-1131.
Popescu, D.C., A.J. Ham, and B.H. Shieh. 2006. Scaffolding protein INAD regulates deactivation of vision by promoting phosphorylation of transient receptor potential by eye protein kinase C in Drosophila. *The Journal of neuroscience : the official journal of the Society for Neuroscience*. 26:8570-8577.
Rabenstein, R.L., N.A. Addy, B.J. Caldarone, Y. Asaka, L.M. Gruenbaum, L.L. Peters, D.M. Gilligan, R.M. Fitzsimonds, and M.R. Picciotto. 2005. Impaired synaptic plasticity and learning in mice lacking beta-adducin, an actin-regulating protein. *The Journal of neuroscience : the official journal of the Society for Neuroscience*. 25:2138-2145.
Ranganathan, R., G.L. Harris, C.F. Stevens, and C.S. Zuker. 1991. A Drosophila mutant defective in extracellular calcium-dependent photoreceptor deactivation and rapid desensitization. *Nature*. 354:230-232.
Roper, K., Y. Mao, and N.H. Brown. 2005. Contribution of sequence variation in Drosophila actins to their incorporation into actin-based structures in vivo. *J Cell Sci*. 118:3937-3948.
Rosenthal, A., L. Rhee, R. Yadegari, R. Paro, A. Ullrich, and D.V. Goeddel. 1987. Structure and nucleotide sequence of a Drosophila melanogaster protein kinase C gene. *EMBO J*. 6:433-441.
Rossner, M., and K.M. Yamada. 2004. What's in a picture? The temptation of image manipulation. *J Cell Biol*. 166:11-15.
Schaeffer, E., D. Smith, G. Mardon, W. Quinn, and C. Zuker. 1989. Isolation and characterization of two new drosophila protein kinase C genes, including one specifically expressed in photoreceptor cells. *Cell*. 57:403-412.
Schmidt, A., and M.N. Hall. 1998. Signaling to the actin cytoskeleton. *Annu Rev Cell Dev Biol*. 14:305-338.
Shieh, B.H., L. Nuzum, and I. Kristaponyte. 2021. Exploring Excitotoxicity and Regulation of a Constitutively Active TRP Ca(2+) Channel in Drosophila. *Fly (Austin)*. 15:8-27.
Shortridge, R.D., J. Yoon, C.R. Lending, B.T. Bloomquist, M.H. Perdew, and W.L. Pak. 1991. A Drosophila phospholipase C gene that is expressed in the central nervous system. *J Biol Chem*. 266:12474-12480.
Smith, D.P., R. Ranganathan, R.W. Hardy, J. Marx, T. Tsuchida, and C.S. Zuker. 1991. Photoreceptor deactivation and retinal degeneration mediated by a photoreceptor-specific protein kinase C. *Science*. 254:1478-1484.

Tsunoda, S., and C.S. Zuker. 1999. The organization of INAD-signaling complexes by a multivalent PDZ domain protein in Drosophila photoreceptor cells ensures sensitivity and speed of signaling. *Cell Calcium*. 26:165-171.

Voolstra, O., J.P. Bartels, C. Oberegelsbacher, J. Pfannstiel, and A. Huber. 2013. Phosphorylation of the Drosophila transient receptor potential ion channel is regulated by the phototransduction cascade and involves several protein kinases and phosphatases. *PLoS One*. 8:e73787.

Voolstra, O., and A. Huber. 2020. Ca(2+) Signaling in Drosophila Photoreceptor Cells. *Adv Exp Med Biol*. 1131:857-879.

Wang, S.J., A. Tsai, M. Wang, S. Yoo, H.Y. Kim, B. Yoo, V. Chui, M. Kisiel, B. Stewart, W. Parkhouse, N. Harden, and C. Krieger. 2014. Phospho-regulated Drosophila adducin is a determinant of synaptic plasticity in a complex with Dlg and PIP2 at the larval neuromuscular junction. *Biol Open*. 3:1196-1206.

Yue, L., and A.C. Spradling. 1992. hu-li tai shao, a gene required for ring canal formation during Drosophila oogenesis, encodes a homolog of adducin. *Genes Dev*. 6:2443-2454.

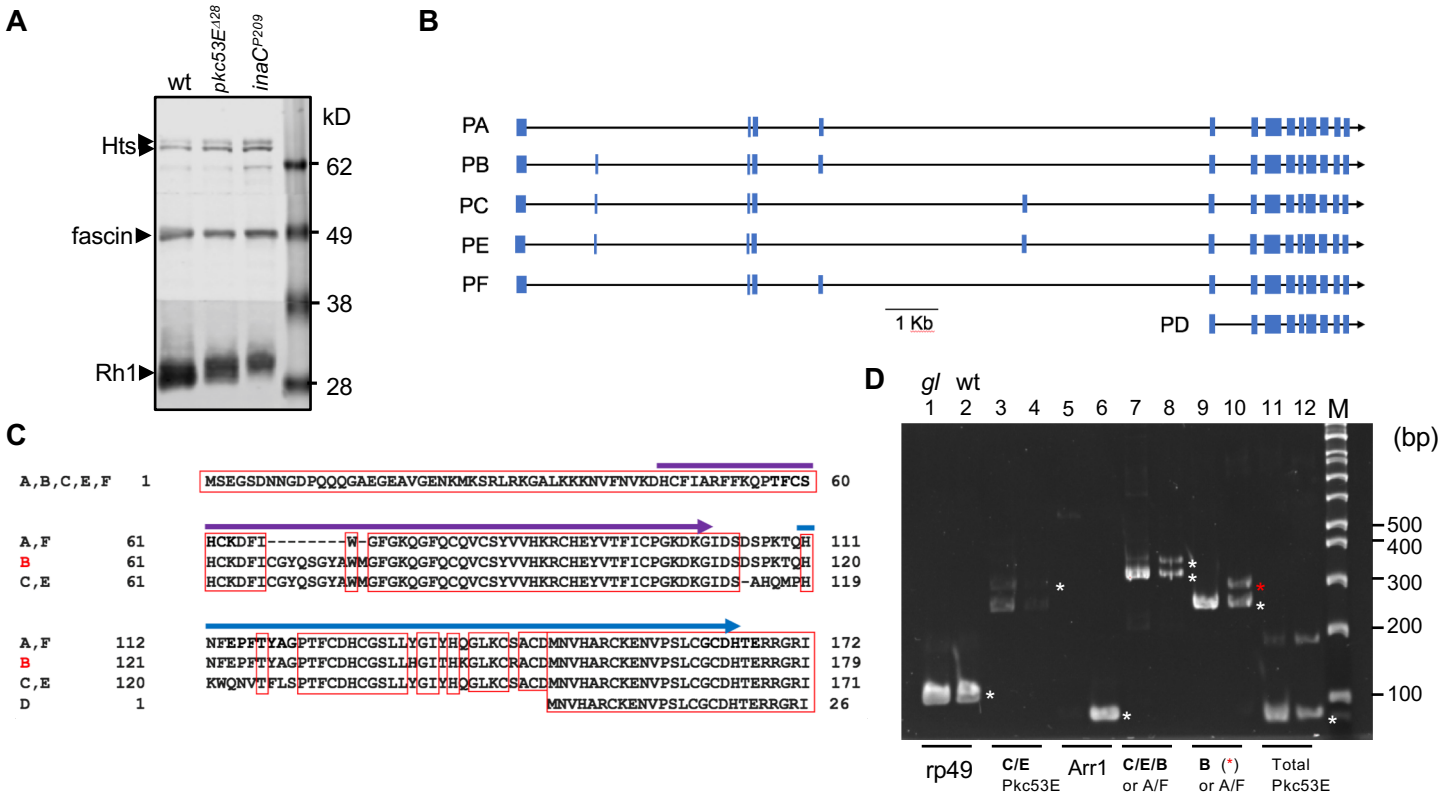
A
wt
pkc53E428
inaCP209
kD
Hts
fascin
Rh1
62
49
38
28
B
PA
PB
PC
PE
PF
PD
1 Kb
C
A,B,C,E,F 1 MSEGSDNNGDPQQQGAEGEAVGENKMKSRLRKGALKKKNVFNVKDHCFIARFFKQPTFCS 60
A,F 61 HCKDFI--------W-GFGKQGFQCQVCSYVVHKRCHEYVTFICPGKDKGIDSDSPKTQH 111
B 61 HCKDFICGYQSGYAWMGFGKQGFQCQVCSYVVHKRCHEYVTFICPGKDKGIDSDSPKTQH 120
C,E 61 HCKDFICGYQSGYAWMGFGKQGFQCQVCSYVVHKRCHEYVTFICPGKDKGIDS-AHQMPH 119
A,F 112 NFEPFTYAGPTFCDHCGSLLYGIYHQGLKCSACDMNVHARCKENVPSLCGCDHTERRGRI 172
B 121 NFEPFTYAGPTFCDHCGSLLHGITHKGLKCRACDMNVHARCKENVPSLCGCDHTERRGRI 179
C,E 120 KWQNVTFLSPTFCDHCGSLLYGIYHQGLKCSACDMNVHARCKENVPSLCGCDHTERRGRI 171
D 1 MNVHARCKENVPSLCGCDHTERRGRI 26
D
gl wt
1 2 3 4 5 6 7 8 9 10 11 12 M
(bp)
500
400
300
200
100
rp49
C/E Pkc53E
Arr1
C/E/B or A/F
B (*) or A/F
Total Pkc53E

Figure 1

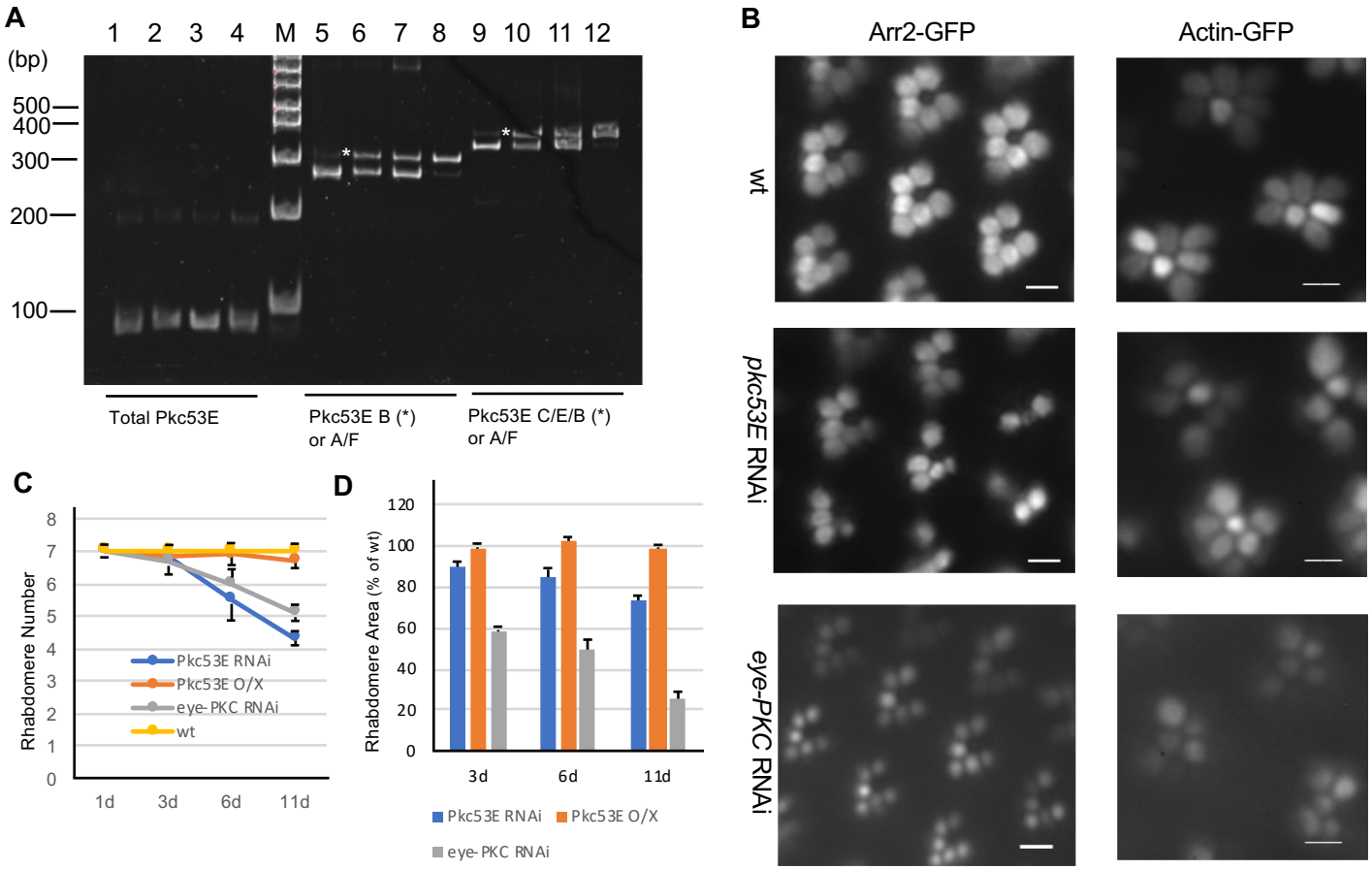
A
1 2 3 4 M 5 6 7 8 9 10 11 12
(bp)
500
400
300
200
100
Total Pkc53E
Pkc53E B (*) or A/F
Pkc53E C/E/B (*) or A/F
B
Arr2-GFP
Actin-GFP
wt
pkc53E RNAi
eye-PKC RNAi
C
Rhabdomere Number
Pkc53E RNAi
Pkc53E O/X
eye-PKC RNAi
wt
1d
3d
6d
11d
D
Rhabdomere Area (% of wt)
3d
6d
11d
Pkc53E RNAi
Pkc53E O/X
eye-PKC RNAi

Figure 2

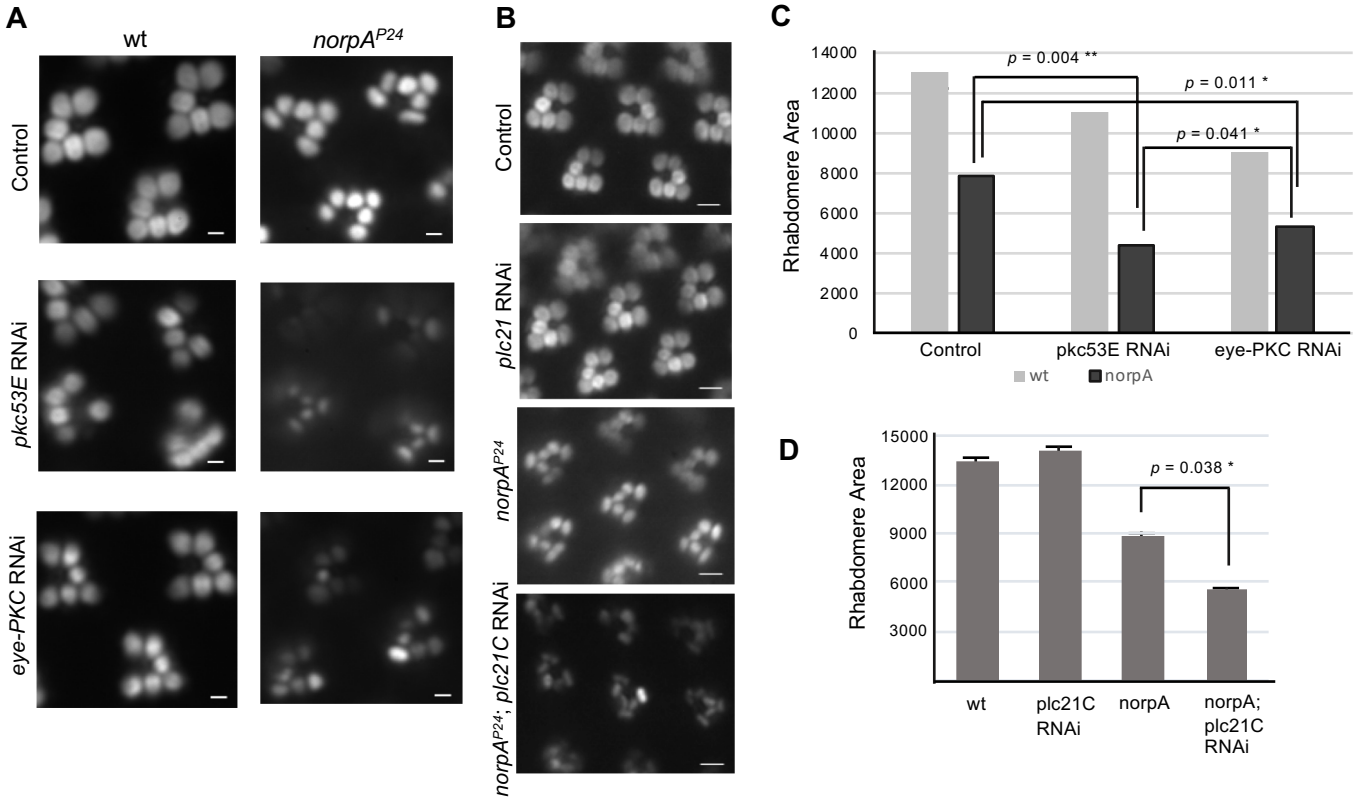
A
wt
norpA^P24
Control
pkc53E RNAi
eye-PKC RNAi
B
Control
plc21 RNAi
norpA^P24
norpA^P24; plc21C RNAi
C
Rhabdomere Area
14000
12000
10000
8000
6000
4000
2000
0
p = 0.004 **
p = 0.011 *
p = 0.041 *
Control
pkc53E RNAi
eye-PKC RNAi
wt
norpA
D
Rhabdomere Area
15000
12000
9000
6000
3000
p = 0.038 *
wt
plc21C RNAi
norpA
norpA; plc21C RNAi

Figure 3

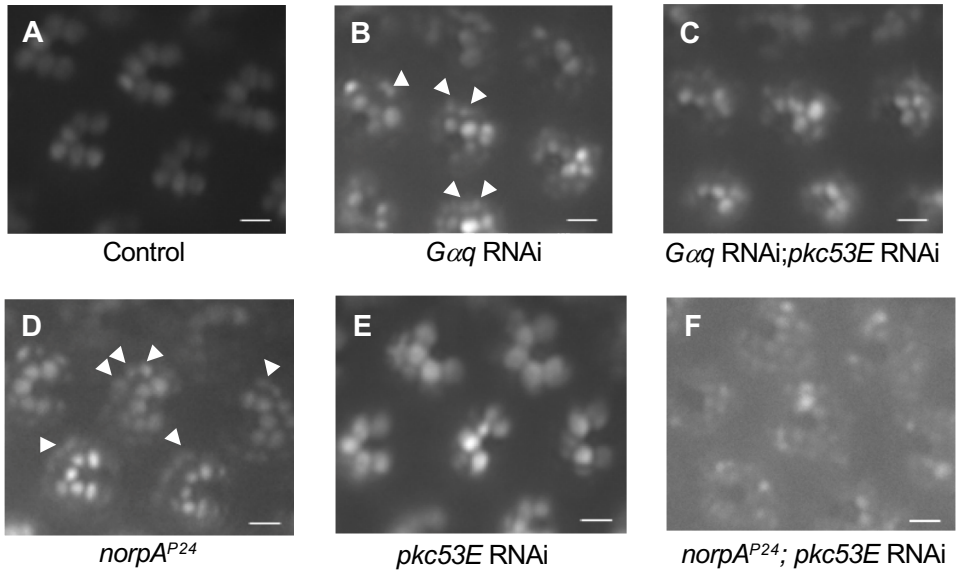
A
Control
B
Gαq RNAi
C
Gαq RNAi;pkc53E RNAi
D
norpA^P24
E
pkc53E RNAi
F
norpA^P24; pkc53E RNAi

Figure 4

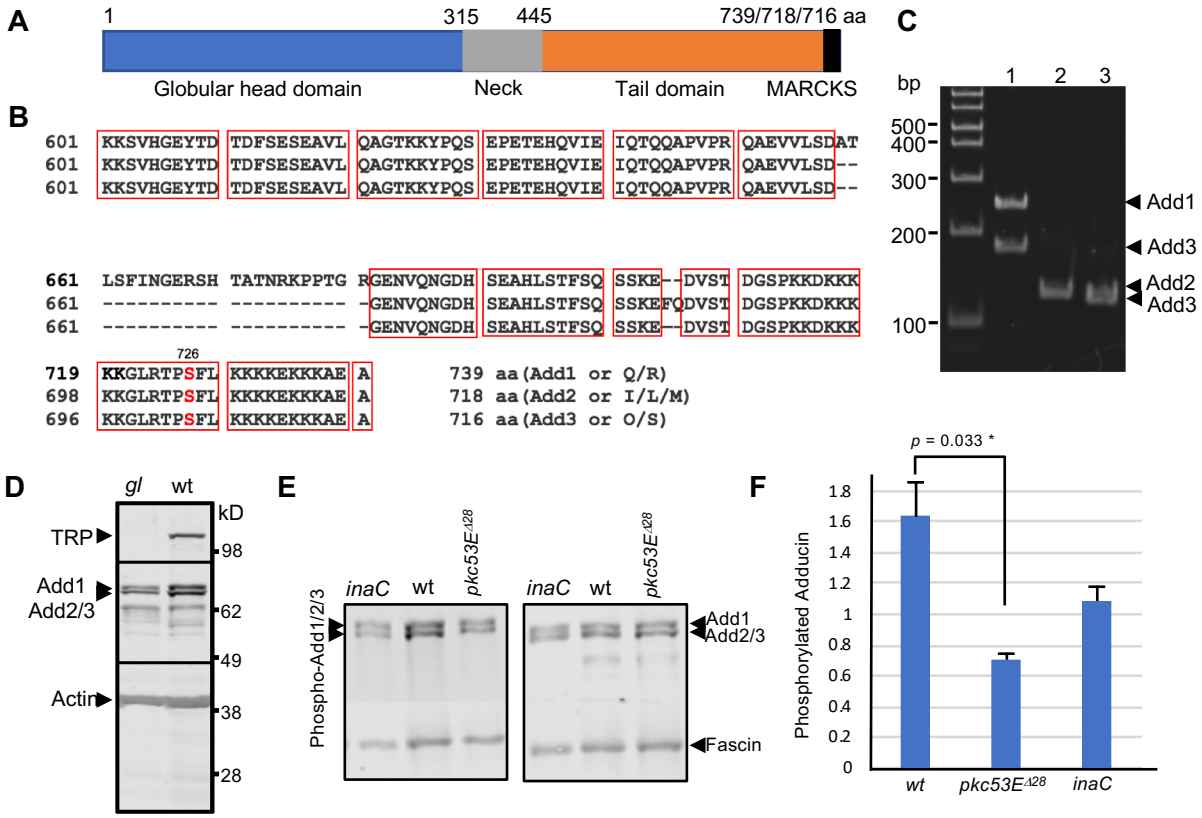
A
1
315
445
739/718/716 aa
Globular head domain
Neck
Tail domain
MARCKS
B
601 KKSVHGEYTD TDFSESEAVL QAGTKKYPQS EPETEHQVIE IQTQQAPVPR QAEVVLSDAT
601 KKSVHGEYTD TDFSESEAVL QAGTKKYPQS EPETEHQVIE IQTQQAPVPR QAEVVLSD--
601 KKSVHGEYTD TDFSESEAVL QAGTKKYPQS EPETEHQVIE IQTQQAPVPR QAEVVLSD--
661 LSFINGERSH TATNRKPPTG RGENVQNGDH SEAHLSTFSQ SSKE--DVST DGSPKKDKKK
661 ---------- ---------- -GENVQNGDH SEAHLSTFSQ SSKEFQDVST DGSPKKDKKK
661 ---------- ---------- -GENVQNGDH SEAHLSTFSQ SSKE--DVST DGSPKKDKKK
726
719 KKGLRTPSFL KKKKEKKKAE A 739 aa(Add1 or Q/R)
698 KKGLRTPSFL KKKKEKKKAE A 718 aa(Add2 or I/L/M)
696 KKGLRTPSFL KKKKEKKKAE A 716 aa(Add3 or O/S)
C
bp
1 2 3
500
400
300
200
100
Add1
Add3
Add2
Add3
D
gl wt
kD
TRP
Add1
Add2/3
Actin
98
62
49
38
28
E
inaC wt pkc53E-Δ28
inaC wt pkc53E-Δ28
Phospho-Add1/2/3
Add1
Add2/3
Fascin
F
p = 0.033 *
Phosphorylated Adducin
1.8
1.6
1.4
1.2
1
0.8
0.6
0.4
0.2
0
wt
pkc53E-Δ28
inaC

Figure 5

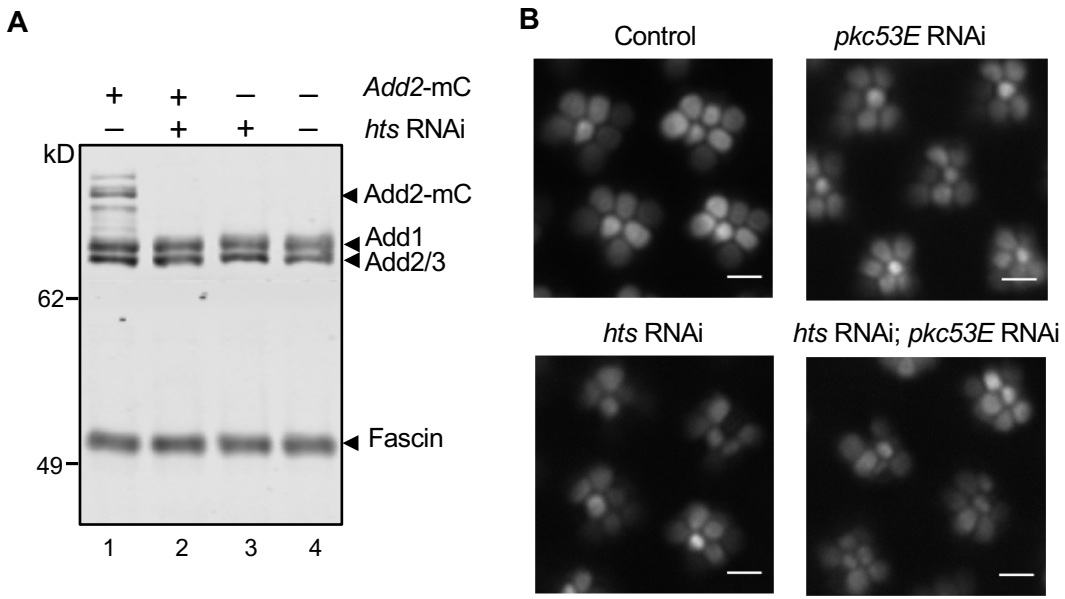
A
+ + – –
Add2-mC
– + + –
hts RNAi
kD
Add2-mC
Add1
Add2/3
62
Fascin
49
1 2 3 4
B
Control
pkc53E RNAi
hts RNAi
hts RNAi; pkc53E RNAi

Figure 6

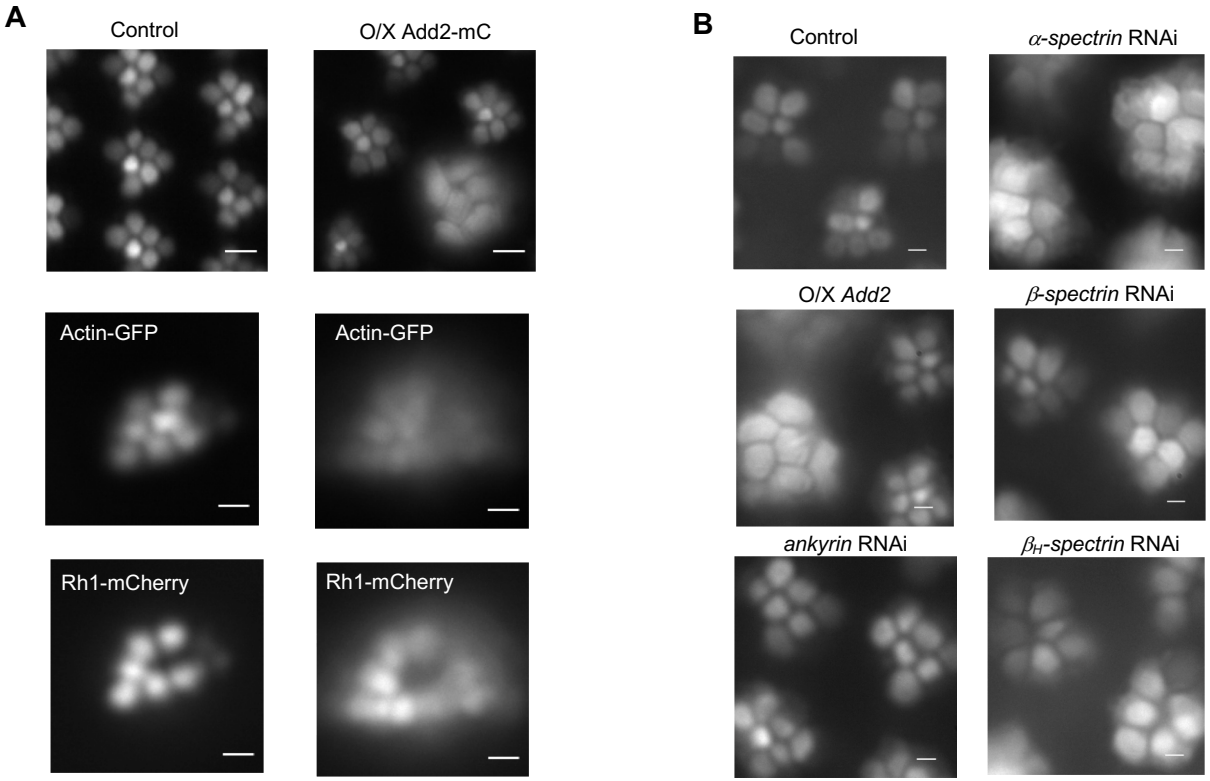
A
Control
O/X Add2-mC
Actin-GFP
Actin-GFP
Rh1-mCherry
Rh1-mCherry
B
Control
α-spectrin RNAi
O/X Add2
β-spectrin RNAi
ankyrin RNAi
βH-spectrin RNAi

Figure 7

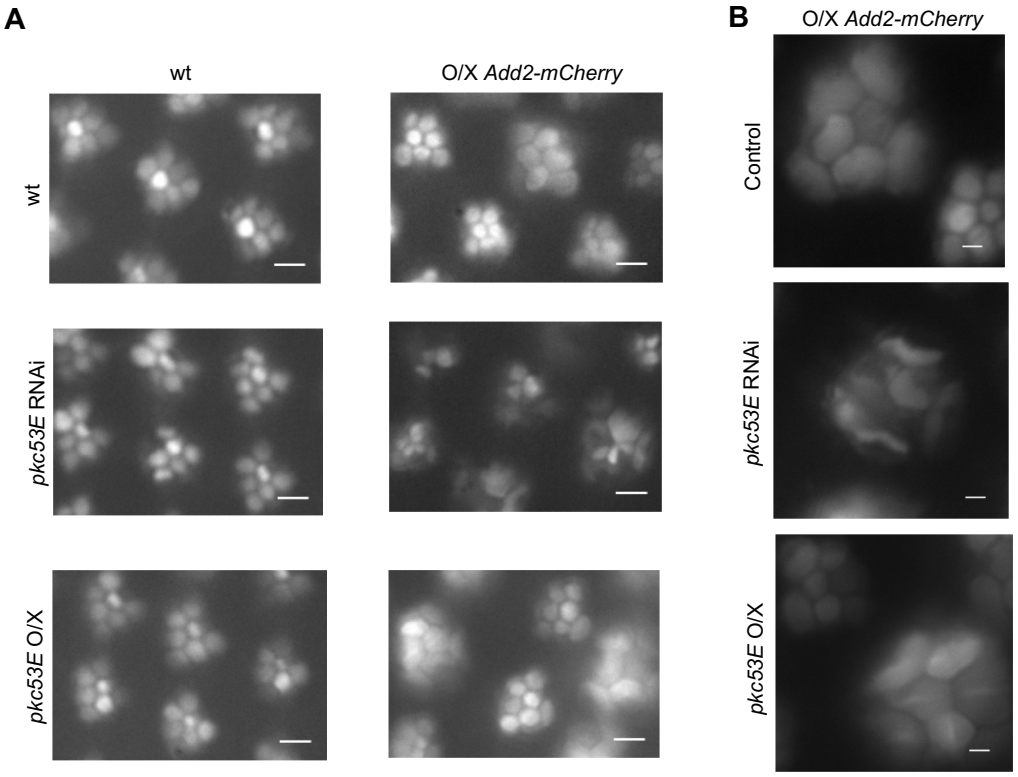
A
wt
O/X Add2-mCherry
wt
pkc53E RNAi
pkc53E O/X
B
O/X Add2-mCherry
Control
pkc53E RNAi
pkc53E O/X

Figure 8

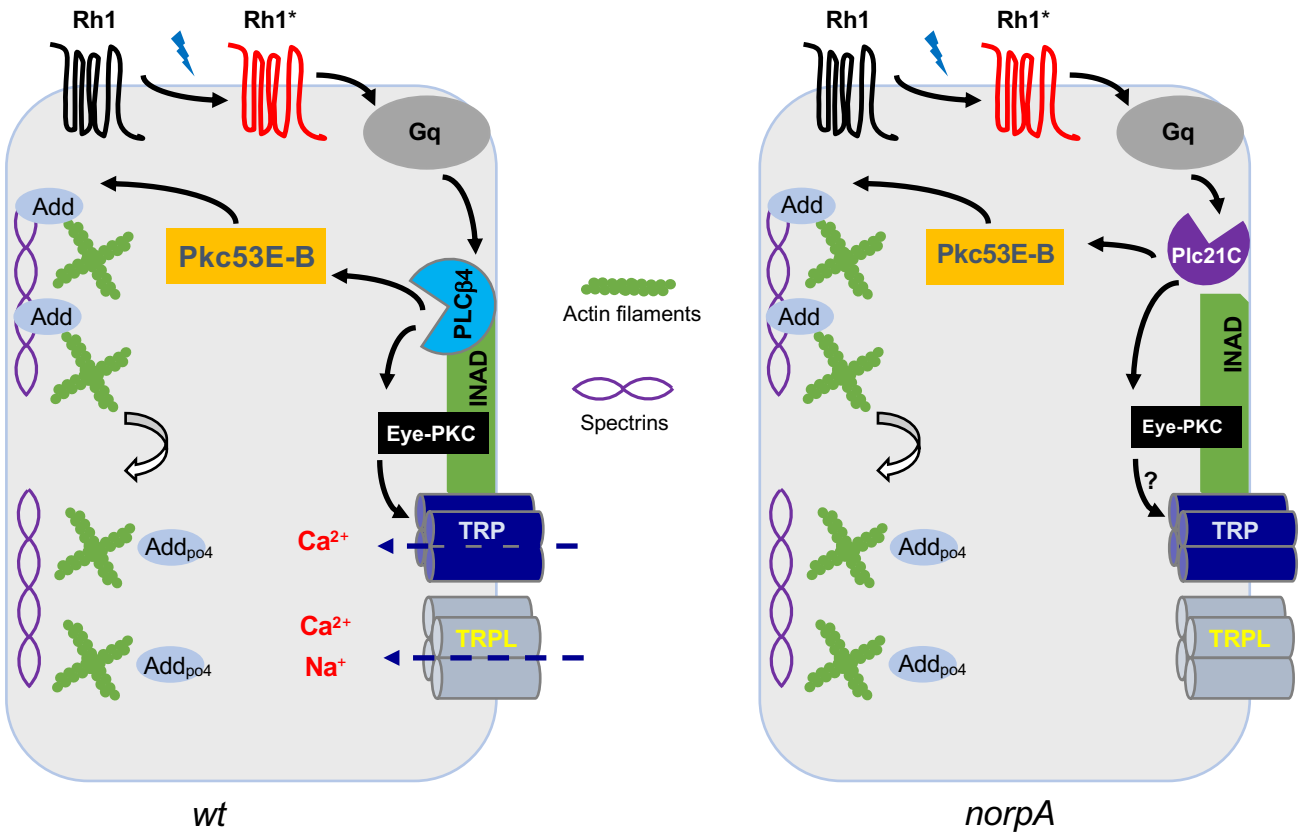
Rh1
Rh1*
Gq
Add
Add
Pkc53E-B
PLCβ4
INAD
Eye-PKC
Add$_{po4}$
Add$_{po4}$
Ca^{2+}
Ca^{2+}
Na^{+}
TRP
TRPL
Actin filaments
Spectrins
Rh1
Rh1*
Gq
Add
Add
Pkc53E-B
Plc21C
INAD
Eye-PKC
?
Add$_{po4}$
Add$_{po4}$
TRP
TRPL
wt
norpA

Figure 9